

Mode delocalization in 1D photonic crystal lasers

Yeheng Wu¹, Kenneth D. Singer^{1,2*}, Rolfe G. Petschek¹, Hyunmin Song², Eric Baer²,
and Anne Hiltner²

¹*Department of Physics, Case Western Reserve University, Cleveland, OH 44106, USA*

²*Department of Macromolecular Science and Engineering, Case Western Reserve University, Cleveland, OH 44106, USA*

kenneth.singer@case.edu

Abstract: We have investigated the formation of in-bandgap delocalized modes due to random lattice disorder as determined from the longitudinal mode spacing in a distributed Bragg laser. We were able to measure the penetration depth, and from transfer matrix simulations, determine how the localization length is altered for disordered lattices. Transfer matrix simulations and studies of the ensemble average were able to connect the gap delocalized modes to localized modes outside of the gap as expected from consideration of Anderson localization, as well as identify the controlling parameters.

© 2009 Optical Society of America

OCIS codes: (230.5298) Photonic crystals; (160.5470) Polymers; (230.1480) Bragg reflectors

References and links

1. P. W. Anderson, "Absence of Diffusion in Certain Random Lattices," *Phys. Rev.* **109**(5), 1492–1505 (1958).
2. S. John, "Strong localization of photons in certain disordered dielectric superlattices," *Phys. Rev. Lett.* **58**(23), 2486–2489 (1987).
3. A. R. McGurn, K. T. Christensen, F. M. Mueller, and A. A. Maradudin, "Anderson Localization In One-Dimensional Randomly Disordered Optical-Systems That Are Periodic On Average," *Phys. Rev. B* **47**(20), 13120–13125 (1993).
4. J. B. Pendry, "Symmetry And Transport Of Waves In One-Dimensional Disordered-Systems," *Adv. Phys.* **43**(4), 461–542 (1994).
5. N. Garcia, and A. Z. Genack, "Anomalous photon diffusion at the threshold of the Anderson Localization Transition," *Phys. Rev. Lett.* **66**(14), 1850–1853 (1991).
6. A. Z. Genack, and N. Garcia, "Observation of photon localization in a three-dimensional disordered system," *Phys. Rev. Lett.* **66**(16), 2064–2067 (1991).
7. P.-E. Wolf, and G. Maret, "Weak localization and coherent backscattering of photons in disordered media," *Phys. Rev. Lett.* **55**(24), 2696–2699 (1985).
8. Y. Lahini, A. Avidan, F. Pozzi, M. Sorel, R. Morandotti, D. N. Christodoulides, and Y. Silberberg, "Anderson localization and nonlinearity in one-dimensional disordered photonic lattices," *Phys. Rev. Lett.* **100**(1), 013906 (2008).
9. J. Topolancik, B. Ilic, and F. Vollmer, "Experimental observation of strong photon localization in disordered photonic crystal waveguides," *Phys. Rev. Lett.* **99**(25), 253901 (2007).
10. T. Schwartz, G. Bartal, S. Fishman, and M. Segev, "Transport and Anderson localization in disordered two-dimensional photonic lattices," *Nature* **446**(7131), 52–55 (2007).
11. M. P. V. Albada, and A. Lagendijk, "Observation of Weak Localization of Light in a Random Medium," *Phys. Rev. Lett.* **55**(24), 2692–2695 (1985).
12. J. U. Nöckel, and A. D. Stone, "Ray and wave chaos in asymmetric resonant optical cavities," *Nature* **385**(6611), 45–47 (1997).
13. H. Cao, "Review on latest developments in random lasers with coherent feedback," *J. Phys. Math. Gen.* **38**(49), 10497–10535 (2005).
14. L. Sanchez-Palencia, D. Clément, P. Lukan, P. Bouyer, G. V. Shlyapnikov, and A. Aspect, "Anderson localization of expanding Bose-Einstein Condensates in Random Potentials," *Phys. Rev. Lett.* **98**(21), 210401 (2007).
15. V. Baluni, and J. Willemsen, "Transmission of acoustic waves in a random layered medium," *Phys. Rev. A* **31**(5), 3358–3363 (1985).
16. D. R. Smith, R. Dalichaouch, N. Kroll, S. Schultz, S. L. McCall, and P. M. Platzman, "Photonic Band-Structure And Defects In One And 2 Dimensions," *J. Opt. Soc. Am. B* **10**(2), 314–321 (1993).

17. M. A. Kaliteevski, D. M. Beggs, S. Brand, R. A. Abram, and V. V. Nikolaev, "Statistics of the eigenmodes and optical properties of one-dimensional disordered photonic crystals," *Phys. Rev. E Stat. Nonlin. Soft Matter Phys.* **73**(5), 056616 (2006).
18. S. Zhang, J. Park, V. Milner, and A. Z. Genack, "Photon Delocalization Transition in Dimensional Crossover in Layered Media," *Phys. Rev. Lett.* **101**(18), 183901 (2008).
19. K. D. Singer, T. Kazmierczak, J. Lott, H. Song, Y. H. Wu, J. Andrews, E. Baer, A. Hiltner, and C. Weder, "Melt-processed all-polymer distributed Bragg reflector laser," *Opt. Express* **16**(14), 10358–10363 (2008).
20. T. Kazmierczak, H. Song, A. Hiltner, and E. Baer, "Polymeric One-Dimensional Photonic Crystals by Continuous Coextrusion," *Macromol. Rapid Commun.* **28**(23), 2210–2216 (2007).
21. E. Baer, J. Kerns, and A. Hiltner, *Processing and Properties of Polymer Microlayered Systems*, Structure Development During Polymer Processing (Kluwer Academic Publishers, The Netherlands, 2000), pp. 327–344.
22. F. Koyama, Y. Suematsu, S. Arai, and T. E. Tawee, "1.5-1.6- μ m Galnsp/Inp Dynamic-Single-Mode (Dsm) Lasers With Distributed Bragg Reflector," *IEEE J. Quantum Electron.* **19**(6), 1042–1051 (1983).
23. J. L. Jewell, Y. H. Lee, S. L. McCall, J. P. Harbison, and L. T. Florez, "High-Finesse (Al,Ga)As Interference Filters Grown By Molecular-Beam Epitaxy," *Appl. Phys. Lett.* **53**(8), 640–642 (1988).
24. D. I. Babic, and S. W. Corzine, "Analytic Expressions For The Reflection Delay, Penetration Depth, And Absorptance Of Quarter-Wave Dielectric Mirrors," *IEEE J. Quantum Electron.* **28**(2), 514–524 (1992).
25. P. Yeh, *Optical Waves in Layered Media*, Wiley Series in Pure and Applied Optics (Wiley, 1998).
26. R. G. Petschek, Y. Wu, and K. D. Singer, (unpublished).

1. Introduction

Anderson localization is a concept in the physics of solids dealing, for example, with a transition from metal to insulator due to multiple scattering of electronic wave functions from random disorder in an otherwise periodic potential resulting from interference of locally scattered waves [1]. The analogous, photon localization in disordered photonic crystals (PhC) has also received considerable theoretical attention during the last decade [2–4]. Early microwave measurements demonstrated photon localization in a disordered system [5, 6]. A number of experiments on photon localization have been carried out on 2 or 3 dimensional systems [5–10]. Observation of both weak [7, 11] and strong photon localization [9] have been found in coherent back scattering experiments. Localization in random media have found application in the study of random lasers [12, 13].

In one dimension (1D), Anderson localization has been studied in electrons, matter waves [14], photons [8], and acoustic waves [15]. In a perfectly periodic dielectric material in 1D PhC, a reflection band appears as a photonic bandgap. Within the bandgap, light is localized as coherent reflection attenuates the light penetrating the structure [3, 7]. Defects in a PhC structure lead to localized defect modes within the bandgap [16]. In contrast, theory and simulations have predicted that a loss of coherent reflection in disordered structures resulting in delocalization of the optical mode as it penetrates the PhC structure [17, 18].

In this work, we study Anderson localization in the case of a 1D disordered lattice by studying the phase delay associated with the longitudinal mode separation in a polymer distributed Bragg laser [19]. We have confirmed that, indeed, the optical mode in the Bragg mirrors becomes delocalized in the presence of disorder, and we were able to quantify the corresponding delocalization. Through transfer matrix theory and simulations, we were able to study this delocalized mode and its connection to Anderson localization outside of the bandgap in keeping with Pendry's analysis [4]. We are able to observe agreement between transfer matrix theory and experiment for disorder induced delocalization within the bandgap by studying the phase delay of the reflected wave. We were also able to quantify the disorder induced localization outside of the bandgap by studying the transmission spectrum of the Bragg mirrors, and to theoretically identify three parameters that control the localization in such reflectors.

2. Experiment

Recently, we reported on all-polymer surface emitting distributed Bragg reflector lasers fabricated using a roll-to-roll compatible melt process [19]. In addition to their fundamental interest, such reflectors are of interest as they may find practical application in low cost photonic devices. The lasers are produced from two 128-layer (i.e. 64 bilayers each) co-

extruded polymer films and a polymer core layers containing laser dyes sandwiched between the Bragg reflectors. The polymers used to make multilayer Bragg mirrors were poly(methyl methacrylate) (PMMA, $n = 1.49$) and polystyrene ($n = 1.585$). The core layer consists of Rhodamine 6G dye doped into a 30/70 blend of PMMA and poly(vinylidene fluoride-co-hexafluoropropylene) with a refractive index of 1.40. The core films were fabricated in various thicknesses with a dye concentration of $5.4 \times 10^{-3} \text{M}$.

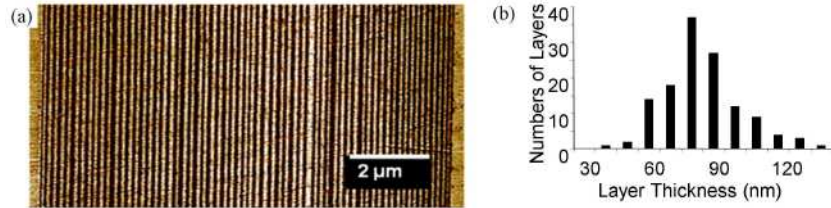


Fig. 1. (a) Atomic force micrograph of the cross section of the multilayer polymer film. (b) Statistic on the layer thicknesses. The layer thickness variation is 22%.

The layer thicknesses comprising the polymer Bragg mirrors were measured using atomic force microscopy (AFM) of the cross section, with a typical cross section shown in Fig. 1(a). Even though the multilayer film has considerable thickness fluctuations (Fig. 1b), it exhibits a clear reflection band as shown in Fig. 2a or Fig. 3a (the difference in these two figures is that there dye absorption centered at around 525nm contributes in Fig. 2a, but not 3a.) These fluctuations occur due to the co-extrusion process, where layer multiplication is used to make the large number of layers [20]. The viscosities of the two melted polymer fluids were well matched by controlling their temperature. However, remaining rheological differences, edge effects during melt spreading in the layer-multiplication dies, and path-length differences in the dies create fluctuations in the layer thickness [21].

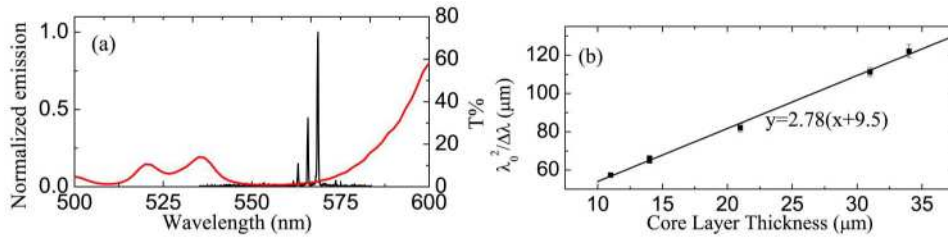


Fig. 2. (a) Typical emission spectrum of the micro-resonator laser (black) superimposed on the DBR stack transmission spectrum (red). (b) The relationship between core layer thickness and the reciprocal of the mode spacing. Solid line is the linear fitting.

The output longitudinal modes from the samples were carefully recorded using an image intensified CCD spectrometer, with an example given in Fig. 2(a). The optical setup and pump laser were described in ref [19]. For various core thicknesses, we observed different modes, which were determined by the round trip time as related to the length of the cavity (L_{eff}).

$$\lambda_0^2 / \Delta\lambda = 2n_{eff}L_{eff} \quad (1)$$

The effective cavity length comprises the optical length (thickness) of the core layer, but also includes the penetration of the mode into the reflective Bragg structures.

$$L_{eff} = L_{core} + 2L_p \quad (2)$$

where L_p is the penetration length. Figure 2(b) is a plot of the mode spacing versus core thickness. Fitting using Eq. (1) and (2), we found the average L_p is $4.8 \pm 0.3 \mu\text{m}$ with $n_{eff} =$

1.39±0.04 in reasonable agreement with the core refractive index of 1.43 especially considering that the core layer contribution to the effective index varies with core thickness as well. Since the thickness of the 128-layer film is approximately 10.8µm, significant penetration of the mode into each Bragg mirror is apparent.

3. Simulation and discussion

Light penetration into mirrors has been previously described [22, 23]. The penetration depth is related to the phase dispersion and to the reflection delay. The former relationship can be written as [24]

$$L_p = \frac{\partial \Delta \phi}{2 \partial k} = - \frac{\lambda^2}{4 \pi n} \frac{\partial \Delta \phi}{\partial \lambda} \quad (3)$$

where $\Delta \phi$ is the phase between the reflected and incident wave. The latter relationship is rather complicated, since in a periodic structure, the phase shift of the reflected wave is based on the superposition of the waves reflected from all the interfaces. However, the delay can be calculated by considering a complex transfer matrix calculation [25]. Calculations were carried out both by assuming a perfectly periodic structure as well as using the actual layer thicknesses as determined from the image in Fig. 1(a). The results are given in Fig. 3. Figure 3(a) depicts the transmission spectrum as calculated for the perfect and “real” films. Regardless of the absorption of the dye molecule in Fig. 2(a), the spectrum in Fig. 3(a) agrees only qualitatively with the measured transmission spectrum in Fig. 2(a) due to variation of the layer thicknesses across the surface of the film and our inability to measure the thickness at the exact spot where the lasing experiments were carried out. Thus, the cross section depicted in Fig. 1a is not the actual laser mirror area, merely taken from the same film. Figure 3(b) and 3(c) depict the penetration lengths calculated using Eq. (3) and the reflectance spectra for a perfect and the “real” film. It is seen that the penetration length in the mid-bandgap region for the perfect film is less than 1 µm while for the “real” film it is between 3 and 4 µm. Clearly the “real” film calculation is much closer to the value from the measured data, and considering the surface variation, is in reasonable agreement. Note should be made here that outside the bandgap, where the reflection is weak, Eq. (3) is invalid simply because the phase of the reflected wave is not the only factor that determines the penetration.

Outside the bandgap, Anderson localization will occur because of the presence of disorder. Pendry has reviewed how the localization length is related to the transmittance, $l_{loc} = -L/\ln T$ showing that Anderson localization leads to delocalized modes in the bandgap and localized modes outside [4]. Here L is the size of the system and T is the transmittance, which can be measured or calculated using the transfer matrix method for any chosen realization of a random system.

Since our measurement was based on many different films, it is suitable to study the large ensemble average. Pendry indicated how to relate the average of the inverse transmittance to a 3×3 matrix $\langle X^{(2s)} \rangle$, which is the average of the symmetric direct product of the transfer matrix with itself. One of the components of the product of N such average transfer matrices is the average inverse transmittance for a stack of N bilayers. For sufficiently large N all components of this product are dominated by the eigenvalue of this matrix having the largest absolute value, as well as its eigenvector. In consequence a definition of the localization length can be taken to be, $l_{loc} = P/t$, where P is the (average) period of the system or average bilayer thickness and $t = \ln(y_{max}^{(2)})$ where $y_{max}^{(2)}$ is the eigenvalue of $\langle X^{(2s)} \rangle$ for which t has the largest real part.

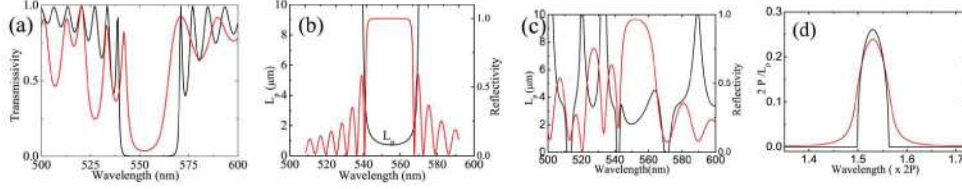


Fig. 3. (a) Transmission spectrum of a perfect film (black) and a real film (red). (b) The effective penetration length (black) calculated from Eq. (3) and reflection spectrum (red) of a “perfect” film. (c) The effective penetration length (black) calculated from Eq. (3) and reflection spectrum (red) of the “real” film. (d) The inverse of localization length for a “perfect” (black) and “real” (red) disordered multilayer polymer film by calculating the largest eigenvalue of the average transfer matrix. P is the average bilayer thickness. The refractive indices used in the calculation are 1.49 and 1.585. In our real system, $2P \sim 370\text{nm}$.

The matrix $\langle X^{(2s)} \rangle$, assuming that layers have equal average and these thicknesses have small, independently distributed Gaussian variations in layer thickness x so that $\langle x \rangle = \bar{x}$ and $\langle (x - \bar{x})^2 \rangle = \sigma^2$, was calculated from the ordinary transfer matrix for dielectric layers using $\langle \exp(ikx) \rangle = \exp(ik\bar{x}) \exp(-\sigma^2 k^2 / 2)$. The determinantal equation for the eigenvalue was calculated using Mathematica. Assuming that $a = (n_1 - n_2) / (n_1 + n_2)$, the difference between the indices of the two layers divided by their sum, is small and $\lambda \ll P/a$, expansion of this equation for small t , and a shows results in [26]

$$\left(1 + \frac{1}{6}(p^2 - \kappa^2)\right)t^3 + s\left(2 - \frac{1}{2}\kappa^2\right)t^2 + t(\kappa^2 - p^2) - \kappa^2 s = 0. \quad (4)$$

In writing the equation in this form we identified the critical physical parameters, $\kappa = 2a \sin(nP / 2\lambda) + O(a^3)$ which is related to the localization length of the perfect PhC and $s = 1 - \exp(-8(\pi\sigma n / \lambda)^2) + O(a^2)$, characterizing the disorder, and $p = \sin(\pi nP / \lambda)$ characterizing the difference between the wavelength and the wavelength at the center of the band gap of the perfect PhC. In this limit the localization behavior can be deduced from this cubic equation with the t^3 , t terms giving the band gap of the perfect PhC, the t^2 term giving the decrease due to the decreased coherence of reflection, and the constant term giving the scattering that results in localization outside the gap. Similar (but algebraically more complex) equations can be deduced with more general assumptions.

In Fig. 1b, the statistics on the multilayer film cross section gives $\sigma = 0.22\bar{x}$. The inverse localization length (e.g. $t/2$) of a perfect and real film as calculated from Eq. (4) is given in Fig. 3(d). This figure clearly depicts both the increased localization outside of the gap and the delocalization inside the gap. Note that significant enhanced localization is observed only over a limited region near each band edge.

We can also examine the intensity distribution throughout the layers. Assuming the light is incident from the left. Figure 4 depicts the results of our numerical transfer matrix calculations on a perfect film (Fig. 4a), and a specific realization of a disordered film (Fig. 4(b)). In Fig. 4(a), intense bands near the band edge can be easily seen reflecting the enhanced density of photonic states at the band-edge. In Fig. 4(b), the large intensity regions (red spots) are seen to be more localized, reflecting Anderson localization. The appearance of the localized fields outside of the gap is consistent with the results depicted in Fig. 3(d), except that in Fig. 3(d) average values are given. This is more clearly verified in Fig. 4(c) as photon localization is enhanced in the presence of disorder, which is shown in the figure by narrowed peaks. Inside the reflection band, the decay is non-exponential as would be generally expected in a disordered system as, shown in Fig. 4(d). The mode penetrates further and thus is less

localized, which is also consistent with conclusion drawn from Fig. 3(d). The phase delay calculated from the laser modes includes the phase accumulated over the nonexponential section beyond layer 60 in Fig. 4(d).

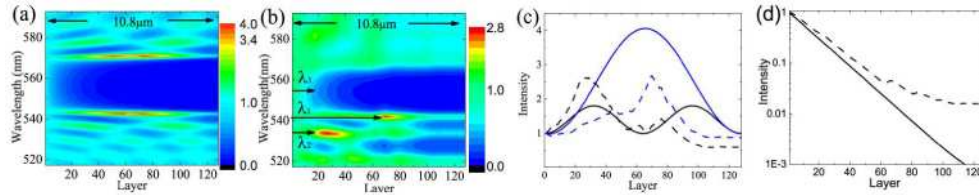


Fig. 4. Transfer matrix calculations of the intensity distribution in a (a) “perfect” 128 layer film, and (b) the “real” disordered 128 layer film. Part (c) plots the intensity against the position outside the band gap. Solid curves: perfect structure; dashed curves: real film with disorder; black curves for wavelength λ_2 denoted in (b); blue curves: at wavelength λ_1 . Part (d) plots the exponential decay (perfect film, solid line) non-exponential decay (real film, dashed curve) behavior of the intensity inside band gap (λ_3).

Thus, we have found both experimentally and theoretically that the disorder introduced into the periodic structure causes the penetration depth to increase well inside the bandgap of the corresponding perfect mirror. We note that the penetration into the layers within the reflection band as deduced from the phase delay reflected in the longitudinal mode spacing has, qualitatively, the same trend as photon delocalization/localization as determined by the energy distribution derived from two types of transfer matrix calculations. The details of this calculation and the relationship between them will be described in a later publication [26].

4. Conclusion

In summary, our observation of delocalization using longitudinal modes in a laser which we have related to Anderson localization in disordered 1D PhCs opens a new experimental path to study and measure Anderson localization in disordered media. The internal photoluminescence and amplified luminescence is a way of injecting photons into the structure and examining localization. The disorder decreases the coherent reflections well inside the band gap of the perfect mirror but localizes light close to the band edge. The enlargement of the effective penetration depth calculated by phase dispersion is the result of photon delocalization inside the bandgap when disorder is introduced into the 1D system. Our theoretical treatment has also revealed the parameters that characterize a somewhat random PhC.

Acknowledgement

The authors are grateful to the National Science Foundation for financial support under the Science and Technology Center for Layered Polymer Systems under grant number 0423914 and the National Science Foundation Materials World Network under grant number DMR-0602767.